A ROBUST METHOD FOR VISION-BASED SEAM TRACKING IN ROBOTIC ARC WELDING

Jae Seon Kim*, Young Tak Son*, Hyung Suck Cho* and Kwang Il Koh**

* Department of Mechanical Engineering
Korea Advanced Institute of Science & Technology
373-1 Kusongdong, Yusunggu, Taejon, Korea

** R&D Complex, Lucky-Goldstar
533, Hogaedong, Dongangu, Anyang, Kyongkido, Korea

ABSTRACT

This paper presents a robotic seam tracking system which is aimed at achieving robustness against some welding noises such as arc glares, welding spatters, fume etc.. In particularly, a syntactic analysis is used to improve the extraction reliability of the joint features. The joint features thus obtained are used to extract the 3-dimensional information of the weld joint and then achieve the robot path correction. To show the performance of the developed system, a series of experiments on joint feature detection and robotic seam tracking are conducted for different types of weld joints. The results exhibit that the system is very robust to various welding noises as well as variations in appearance of weld joint and workpiece.

1. INTRODUCTION

Although the development of robotic arc welding systems has rapidly progressed until recently, the robotization of arc welding process still suffers from several problems. These include (1) real-time correction to the pre-taught welding path, which needs to be achieved to compensate for the fixturing inaccuracies of workpiece to be welded, the dimensional variations, and in-process thermal distortions, and (2) appropriate change in welding parameters, which needs to compensate for any variations in the joint geometry. Extensive researches on the usage of visual feedback signal have been done to solve these fundamental problems. However, most early vision-based robotic welding systems [1-3] have been proved still to yield several limited functionality and flexibility for the practical use.

In this paper, an adaptive robotic arc welding system is developed with a vision sensor for measuring the detailed geometric features of weld joint to be welded, and then achieving the robot path correction. The goal of the work is to achieve the robustness to variations in joint configuration, joint size as well as the optical disturbances such as arc glares, welding spatters and smoke. To achieve the goals, two separate vision processing algorithms are developed for the joint modeling and the joint feature detection, respectively. The joint model made before welding is used as a template model for searching the joint features during welding.

In particularly, a syntactic approach (see [4]) is adopted to enhance the detectability of significant joint features. Sicard *et al.* [3] have recently used a syntactic approach for recognition and tracking of weld joints. In principle, the method appears to be efficient, but is apt to to fail when input data are heavily degraded due to some intensive welding noises. In comparison with the work for the 1-dimensional range data obtained by the laser spot scanner, the syntactic method used in this paper is developed for a 2-dimensional image of the striped laser light. To cope with less favorable situation in processing of the stripe images, the syntactic algorithm is further refined. Several new junction primitives and production rules are defined to treat the noisy stripe data and also tackle a variety of variations in welding joint configuration. In addition, a more strictly defined template matching method is used to improve the detection reliability of weld joint features.

2. SYSTEM DESCRIPTION

As shown in Fig.1, the overall visual seam tracking system is composed of two modules: a robot control module and a vision processing module. The robot control system consists of two units: main processing unit and joint servo unit. The main processing unit operates major processing such as coordinate transformation for trajectory control in cartesian coordinates, sensory feedback control for seam tracking etc.. The joint servo unit receives the angular motion vector at each sampling period of 16ms from the main processing unit, and controls AC servo motor of each axis. The vision processing module analyzes the image data obtained from the vision sensor to recognize the joint features. This module communicates with the

0-7803-2722-5/95 $4.00 © 1995 IEEE

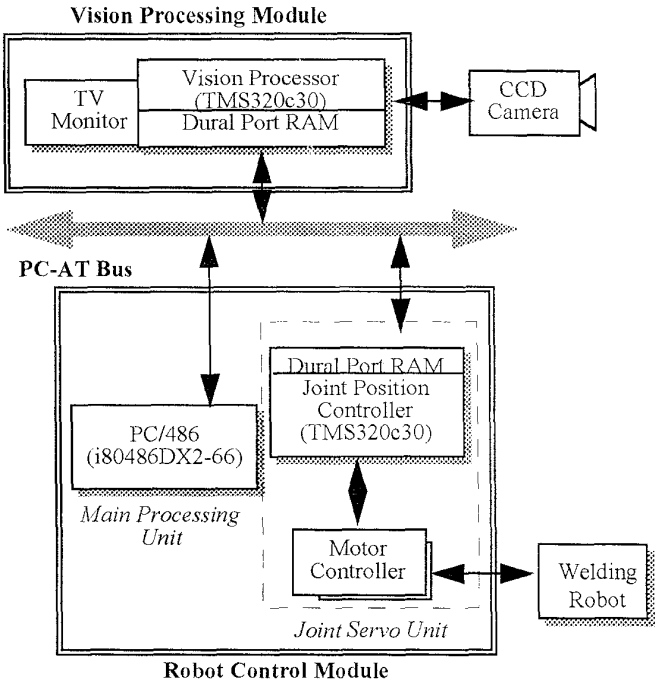

Fig.1. The overall system hardware architecture

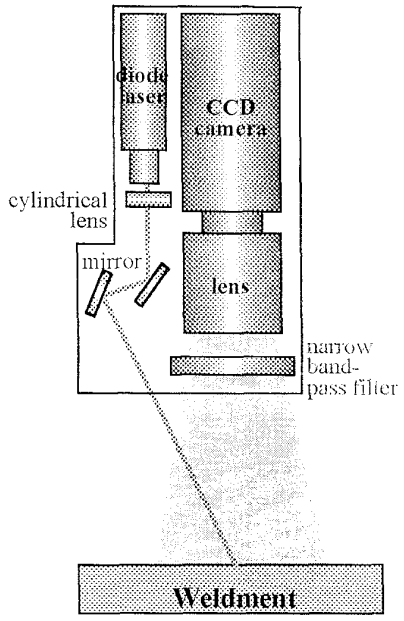

Fig.2. Configuration of the vision sensor

main processing unit of the robot control module through PC-AT bus at every sensory feedback sampling period.

The vision sensor consists of a CCD image sensor and a compact optical projection system that generates a plane of light beam, as shown in Fig.2. The camera is fitted with a narrow-band optical interference filter having a spectral bandpass of 10nm centered at the 690nm. The narrow-band interference filter efficiently removes much of the ambient and welding arc light from the image. The optics is so arranged that one pixel in the image plane corresponds approximately to 0.08mm on a focused object. As a source of light, the 25mW laser diode emitting at 690nm is used. From the stripe image data obtained from the sensor, the 3-dimensional layout of workpiece can be obtained based on a principle of active triangulation ranging (see [5]).

3. VISION PROCESSING ALGORITHMS

The vision processing algorithm is split into two separate stages. In the first stage, a stripe image with the arc turned off is acquired at the starting point of the weld joint, and then the imaged geometry of the joint profile is modeled. The second stage is operated during welding in which the goal is to track the joint by on-line determining the weld joint features. The joint model obtained in the first step is used as a template model for searching the joint features during welding.

3.1. Joint Modeling

3.1.1. Extraction of raw profile data

The basic idea to extract the laser stripe projected in the image is to convolve the pixel data with a spatial filter such as the second derivative of a Gaussian [6] that only operates in the direction of the columns of the image, because the stripe is approximately parallel to the rows of the image. To enhance the discrimination of the laser stripe from other possible brightness sources such as arc glares and welding spatters, however, the thickness of the stripe is expected to be first estimated (see [8] for detailed explanation on the thickness estimation method). The resulting thickness L_w is then used for dynamic design of the filter in 1-dimension. In order for the filter to run reasonably fast, the following approximation is used:

$$R(i,j) = \sum_{m=-3/2L_w}^{3/2L_w} \omega_m I(i,j+m) \qquad (1)$$

where $I(i,j)$ denotes the pixel value at the image coordinates (i,j) and ω is a filter coefficient that has a mexican hat-like distribution. For a given column, the point of the maximum value among the filter responses R is obtained. If the maximum response is larger than a threshold value, the corresponding position is considered to be the center position of the stripe at the column.

Once the stripe location data are extracted from the input image, the data are grouped into a set of

connected runs. The resulting runs are then fitted to straight line segments by using the polygonal line approximation method (see [7]), the basic idea of which is to find the break points located at the significant orientation changes along the connected run.

Table 1. Shape descriptive labels

	Label	Description
Line Primitives	*speckle*	
	surface	
Junction Primitives	*cp*	
	cu	
	cd	
	gp	
	gu	
	gd	
	up	
	uu	
	ud	
	ap	
	au	
	ad	
	dp	
	du	
	dd	
	bp	
	bu	
	bd	

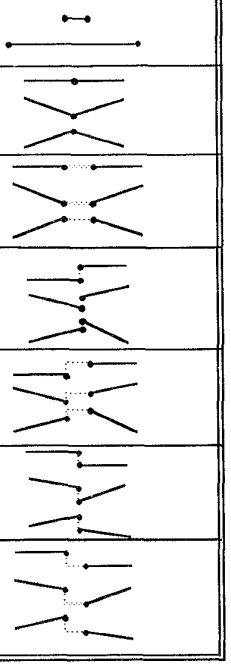

3.1.2. Syntactic Analysis

Pattern representation: The first step of the syntactic analysis is to represent the stripe profile as a string of linguistic words. Each of line segment and junction between two neighboring line segments is assigned a label in accordance with a pre-defined primitive vocabulary. The pattern primitives defined for this work are illustrated in Table 1.

A line segment is assigned the label of "*speckle*" or "*surface*" to its lenghth. A threshold value D_{th} is used to discriminate between speckle line segment and surface one. In addition, eighteen junction labels are defined to characterize the positional arrangement and the orientation change between two adjacent line segments. A threshold value U_{th} is needed for deciding whether there is significant lateral gap between two adjacent line segments, and also another threshold value V_{th} is used for deciding whether there is significant upward or downward transition. Finally, a threshold value P_{th} is used for deciding whether there is significant change in orientation between two adjacent line segments. The labeling process finally yields a string of words that alternate between line segment label and junction label .starting from the leftmost line segment.

Refining of the string: The next step is to refine the string such that only the significant surface segments and junctions remain in the final representation. Starting from the leftmost three words, the string is merged or modified according to the production rules listed in Table 2.

The rules with the expression of $A \rightarrow B$ indicates that the expression A can be replaced by the expression B. The rules falling under the category with the expression of $A \rightarrow\rightarrow B$ replace three words of the expression A by a word of the expression B, which represents a new line segment that connects the starting point of the left line segment and the ending point of the right one in the expression A. The overall meaning of this class of rules is to merge two succeeding line segments contacting each other if the change in orientation between them is small, or two speckle segments succeed each other. Exceptional cases are rules 16 and 18, which are particularly intended for eliminating some excessive speckles that are likely to be yielded around rounded off edges on workpiece.

In the rules with the expression of $A \leftarrow B$, the modification is performed under the particular strategy in the expression B. The rules 20 and 21 are intended for removing some isolated speckles yielded by some optical noises such as intensive arc glares, welding spatters and highlighted spots on workpiece surface. The rules 22, 23 and 24 are particularly considered for enhancing detection accuracy of the joint features that may be disturbed by some unexpected tiny gaps between two significant surfaces or rounded off edges of workpiece. Such unexpected tiny gaps usually occur due to incomplete fixturing and preparation of workpiece or its distortion during welding..

Starting with the first three words in the input string, each rules 1-22 are applied to the words one after another. If a match occurs, the modification is performed according to the matched rule. The modification process is repeated until no more match is made over the string. Finally, rules 23 and 24 are in turn applied to the string to enhance the detection accuracy of intersection points.

3.1.3. Joint Profile Modeling

The next is to model the imaged geometry of the joint to be welded. To do so, the string that survives the revision process is matched to the pre-defined generic models of typical weld joints (see [8] for detailed explanation). If a match is found, the model is recognized as type of the weld joint. Once the joint identification is completed, the locations of the joint features are determined by examining the junctions in the input profile that match with the junctions in the generic model. The extracted joint features constitute template profile of the weld joint. The template is composed of a series of branches, each of which has two components: the length and the angle. It can be

written by

$$T = \{(l_1, \theta_1), (l_2, \theta_2), \cdots, (l_n, \theta_n)\} \quad (2)$$

where n is the number of branches, l is the length of branch, and θ is the angle of branch with respect to the horizontal line.

windowed image (about 250(H) x 200(V) pixels) surrounding the expected stripe location. It is desirable that the expected location of the window center is recognized as the joint center position detected in the previous processing time. The stripe centers are extracted by using the second derivative of a Gaussian filter built in the joint modeling stage. As in the joint modeling stage, the extracted stripe data are fitted to straight lines, and then the incorrectly segmented, missing or overrefined segments are refined through the syntactic analysis.

Table 2. Production rules

Rule No.	Expression
Rule 1 Rule 2 Rule 3 Rule 4	<u*> → <float> <a*> → <d*> → <b*> →
Rule 5 Rule 6	<float> → <break> <g*> →
Rule 7 Rule 8	<cu> → <vertex> <cd> →
Rule 9 Rule 10	<vertex> → <contact> <cp> →
Rule 11 Rule 12	<speckle> → <anyline> <surface> →
Rule 13	<speckle><contact><speckle> →→ <speckle> (if the distance between the start point of the first speckle and the end point of second speckle does not exceed a threshold value (D_{th}))
Rule 14 Rule 15 Rule 16 Rule 17 Rule 18 Rule 19	<speckle><contact><speckle> →→ <surface> (if the distance exceeds a threshold value (D_{th})) <speckle><cp><surface> →→ <speckle><vertex><surface> (if preceded by <break>) →→ < surface><cp><speckle> →→ <surface><vertex><speckle> (if followed by <break>) →→ <surface><cp><surface> →→
Rule 20 Rule 21 Rule 22	<surface><float><speckle> (if followed by <float>) ← remove <speckle> <speckle><float><speckle> (if followed by <float>) ← <surface><vertex><speckle> (if followd by <vertex><surface>) ←
Rule 23	<anyline><vertex><anyline> ← Modify to contact at the intersection point of the extension of first segment and the extension of second segment (if the end point of first segment is not identical to the start point of second segment)
Rule 24	<anyline><cp><anyline> ← Modify to contact at the middle point between the end point of first segment and the start point of second segment (if the end point of first segment is not identical to the start point of second segment)

3.2. Joint Feature Detection During Welding

3.2.1. Extraction of raw profile data

To significantly decrease the vision processing time, the vision processing is conducted on only the

3.2.2. Joint Feature Detection

To extract the joint features, the segmented joint profile is matched with the template profile built in the previous processing time. The goal is to search the best match, which is found when the template is attached to the breakpoints of the input profile such that the total matching cost is minimized.

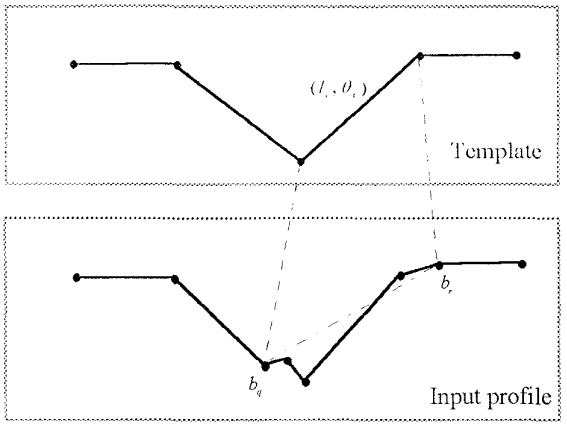

Fig. 3. Template matching

Suppose that the ith branch of the template profile is matched to the breakpoints b_q and b_r of the input profile (see Fig. 3). In this case, the matching cost $C_i(q,r)$ is defined by

$$C_i(q,r) = w_l L_i(q,r) + w_a A_i(q,r) + w_s S_i(q,r) \quad (3)$$

where w_l, w_a and w_s are weighting factors, and $L_i(q,r)$, $A_i(q,r)$ and $S_i(q,r)$ denote the measures of similarity in length, angle and straightness between the pair to be considered for matching, respectively. The total matching cost C is the sum of each the matching cost over all the branches comprising the template profile. If the total matching cost at the best match is smaller than a threshold value, the selected intersection points serve to determine the joint features in the stripe data, and replace the attributes of the template to cope with some possible variations of the joint features in the next incoming image. Therefore, successful tracking of the joint features will be achieved as long as the joint geometry and location are not abruptly changed in large amount. If the match cost is larger than the threshold value, the feedback to the welding robot is bypassed.

4. EXPERIMENTS AND DISCUSSIONS

To investigate the performance of the developed visual system, two types of tests have been carried out by using the actual robotic welding system as in the followings. In each welding experiment, the gas metal arc (GMA) welding has been processed on the workpieces of hot rolled steel 1025.

4.1. The joint feature detection

A series of experiments have been performed for a variety of butt, lap, fillet and vee joints. Fig.4 shows vision processing results for the four joint types.

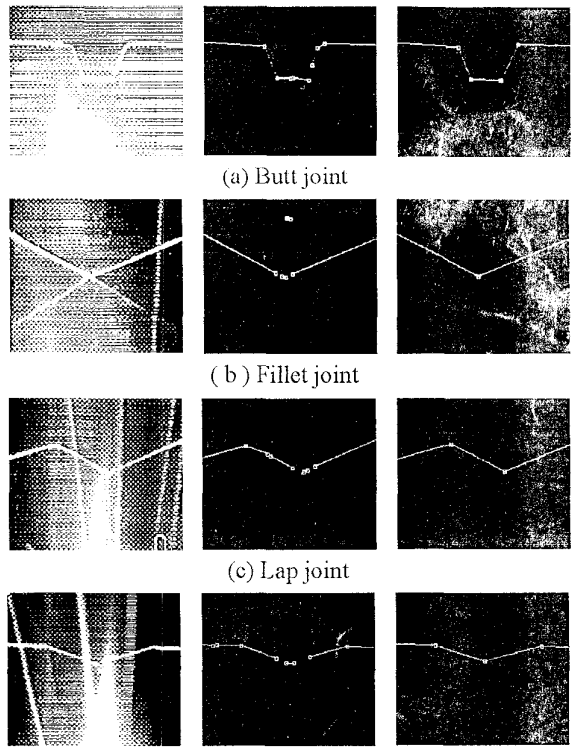

(a) Butt joint

(b) Fillet joint

(c) Lap joint

(d) Vee joint

Fig.4. Detection results of joint features

The stripe images captured from the vision sensor are exhibited in the first column of the figure in which they are obtained with the arc turned on and possess some optical noises caused by arc glares, spatters and so on. To obtain the images with various levels of the optical noises, they were taken from the vision sensor ahead of the welding torch by different distances ranging from 10mm to 50mm. The center image of each row shows a list of line segments obtained by applying the polygonal line approximation after the stripe extraction in which the ending points of each segment are remarked by squares. All of the results exhibit that a number of segments over the number of significant surfaces on the joint are yielded. The right images in each row show the finally detected joint features. Squares indicate the locations of the resulted feature points. All of the results show that the significant joint features were successfully extracted regardless of intensive arc glares or spatters.

In all of the results, the following parameters were

used: $D_{th} = 6$, $U_{th} = 15$, $V_{th} = 10$, and $P_{th} = 20$. From a number of experiments with different parameters, it appeared that choice of parameter P_{th} was most critical to the results. If the value is small, a number of artificial features are generated. This often caused incorrect identification of joint type or inaccurate detection of joint features. The values of thresholds D_{th}, U_{th} and V_{th} need to be varied according to particular geometry of the workpieces to be welded, such as gap size or material thickness.

4.2. The robotic seam tracking

To test the seam tracking ability of the developed system, a number of robotic welding guided by the vision processing results have been conducted on various types of weld joints. One of the results is shown in Fig.5 in which the vee-grooved joint of curved shape on the flat plates ($300mm \times 220mm \times 8mm$) slanted upwards along the welding direction was used. The vision sensor was located ahead of the torch by a distance of 35mm. In the welding experiment, the welding speed and input power was fixed to be $8mm/\text{sec}$ and $3000W$, respectively. This inappropriate welding conditions yielding insufficient penetration were intentionally considered for enhancing the view of the torch positions and the joint configurations in the cross-sections of the weld bead. This figure shows the macro-photographs of the cross-sections of the weld bead at the positions remarked by arrows. The results exhibit that the tracking has been performed with a reasonable accuracy regardless of variations in joint arrangement and groove preparation.

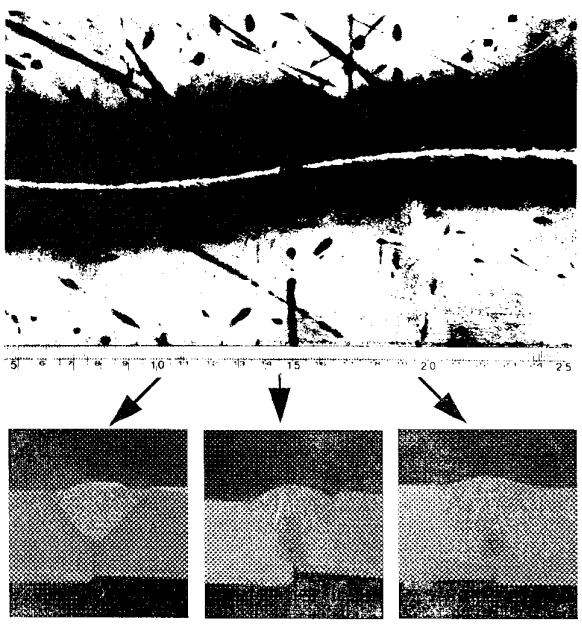

Fig.5. Weld bead after robotic welding: vee joint

5. CONCLUSIONS

In this paper, a robotic seam tracking system which utilizes a structured lighting-based vision sensing technique was presented to achieve robustness to hostile welding environments. In summary, the main features of the developed system include the followings. 1) Reliable recognition of weld joint features can be achieved in the presence of (a) welding optical noises, (b) mutual reflection of laser light onto other surfaces on workpiece, and (c) variations in joint geometry and configuration. 2) A reasonable accuracy in the measurement of 3-dimensional location of joint features and in the seam tracking by welding robot can be obtained: Seam tracking ability of the developed system was measured to be consistently better than $\pm 0.5mm$, which is more than adequate for most GMA welding process. 3) A real time guidance of welding robots can be achieved: The vision sensor could supply profile data of the joint to be weld at a rate of about 7 times per second.

REFERENCES

[1] Clocksin W.F., Bromley J.S.E., Davey P.G., Vidler A.R. and Morgan C.G., An implementation of model-based visual feedback for robot arc welding of thin sheet steel. *Int. J. of Robotics Research* 4, 13-26 (1985).

[2] Agapakis J.E., Visual sensing and knowledge-based processing for automated robotic welding fabrication. *Proc. Int. Computers in Engineering Conf.* 1, 225-231 (1985).

[3] Sicard P. and Levine M.D., Joint recognition and tracking for robotic arc welding. *IEEE Trans. on Systems, Man, and Cybernetics* 19, 714-728 (1989).

[4] Fu K.S., *Syntactic pattern recognition and applications*. Prentice Hall, Englewood Cliffs, NJ (1982).

[5] Popplestone R.J. and Ambler A.P., *Forming body models from range data*. Research Report 46, Department of Artificial Intelligence, University of Edinburgh (1977).

[6] Marr D. and Hildreth E., *Theory of edge detection*. MIT AI Memo 518, Cambridge Mass. (1979).

[7] Pavlidis T. and Horowitz S.L., Segmentation of plane curves. *IEEE Trans. Comput.* 23, 860-870 (1974).

[8] Kim J.S., Son Y.T, Cho H.S and Koh K.I A robust visual seam tracking system for robotic arc welding. *Mechatronics*, to be submitted for publication.